



Solitary wave solutions of coupled nerve fibers model based on two analytical techniques

Waseem Razaq^{1,2} · Arzu Akbulut³ · Asim Zafar² · Melike Kaplan⁴ · M. Raheel²

Received: 14 December 2022 / Accepted: 8 April 2023 / Published online: 14 May 2023

© The Author(s), under exclusive licence to Springer Science+Business Media, LLC, part of Springer Nature 2023

Abstract

This paper focuses on a few innovative solutions to the coupled nerve fibers model. The constructed solutions can be used to expose this model in a noticeable way. The verified solutions are including the trigonometric, exponential, and hyperbolic functions. Utilizing the Mathematica tool, the results are verified. We employed two approaches, named as modified extended tanh expansion and modified $(\frac{G'}{G^2})$ -expansion methods, to obtain the results. We gave the 2-D and 3-D plots of the obtained results. The obtained results are dissimilar from previous results in the literature. The used methods are powerful and effective. The obtained results have potential to be conducive for the model's future development.

Keywords Coupled nerve fibers model · Conformable derivative · Modified extended tanh expansion method · Modified $(\frac{G'}{G^2})$ -expansion method · Solitary wave solutions

1 Introduction

In literature, scientists carry out many physical phenomena in electromagnetic theory, fluid mechanics, physical chemistry, geophysics, fluid motion, nonlinear optics, plasma physics, and their mathematical models are described by NFDEs. These equations have experienced significant several investigations from distinct viewpoints and are frequently utilized in a number of scientific disciplines. There is growing interest in the soliton theory of these equations. Because of this, researchers have studied a wide variety of techniques. Soliton theory has been the subject of extensive research. Numerous applications can be found in many fields, including as quantum theory, biology, plasma physics, electronics theory, solid state physics, and so on. Many kinds of phenomena that occur in nature are modeled using NFDEs. There are several different types of soliton, including periodic, brilliant, dark single, real, trigonometric,

✉ Arzu Akbulut
ayakut1987@hotmail.com; arzuakbulut@uludag.edu.tr

¹ Math Center, House no 87 Rahmanyia Colony, Vehari, Pakistan

² Department of Mathematics, CUI, Vehari Campus, Vehari, Pakistan

³ Department of Mathematics, Faculty of Arts and Science, Bursa Uludag University, Bursa, Turkey

⁴ Department of Computer Engineering, Faculty of Engineering and Architecture, Kastamonu University, Kastamonu, Turkey

hyperbolic, dark-bright, and more. Numerous techniques are used to obtain these kind of solutions such as; extended Jacobi’s elliptic function expansion algorithm (Osman et al. 2021), modified Kudryashov and addendum Kudryashov methods (Zayed et al. 2022), direct similarity reduction scheme (El-Shiekh et al. 2021), modified extended tanh expansion (METH) procedure (Zafar et al. 2021), extended sinh-Gordon equation expansion procedure (Mathanaranjan et al. 2022), and so on. (Ablowitz and Clarkson 1991; Hirota 1971; Weiss et al. 1983; Rezagadeh et al. 2018; Kalim et al. 2018; Tala-Tebue et al. 2018).

Presently a lot of research have been done in the field of optical fibers and nonlinear optical fibers to observe the dynamically behaviour of neural network. For example, the validity of the power law decay distribution checked by using the simulations with a phenomenological model (Lv et al. 2017). A type of switching neural networks based on memristors that have time-varying delays has its finite-time stability issue identified (Ali et al. 2017) and many more (Moore et al. 1978; Tourani et al. 2016; Huang et al. 2018; Tsai et al. 2018). Soliton theory investigated by using analytical methods such as the sub-equation and Bernoulli sub-equation function procedures (Duran et al. 2021), modified sub-equation method (Duran et al. 2021), improved tanh method (Yokus et al. 2022) has attracted attention from all over the world. In this study, we applied different methods to a different model.

The exact soliton solutions are governed of the coupled nerve fibers model by using the improved Riccati equation mapping procedures (Tala-Tebue et al. 2019).

The fundamental focus of the corrent paper is to examine solitary wave solutions to the coupled nerve fibers model based on the METH and modified $(\frac{G'}{G^2})$ -expansion techniques.

Consider the coupled nerve fibers model given as Tala-Tebue et al. (2019):

$$\begin{aligned}
 M[(1 - \eta)\sigma^2 v_{xx} - \eta\sigma^2 u_{xx}] &= R_f CD_t^\alpha v + \gamma v(v - a)(v - 1) \\
 M[(1 - \eta)\sigma^2 u_{xx} - \eta\sigma^2 v_{xx}] &= R_f CD_t^\alpha u + \gamma u(u - a)(u - 1)
 \end{aligned}
 \tag{1}$$

where $v = v(x, t)$ and $u = u(x, t)$ represent the travelling waves profiles, $M = \frac{R_f}{R}$, $\gamma = R_f \frac{G}{(1-a)}$, $\eta = \frac{R_0}{R}$, $R = R_i + R_0$, $a = \frac{V_a}{V_b}$. V_a shows threshold voltage, and V_b represents the Nernst potential. G stands for the total ionic conductance near V_b , and C represents the capacitance. η is the parameter through which two fibers are linearly coupled and σ shows the internodal spacing. If we take $\alpha = 1$, then we get the model met in the literature which is a special case of aforementioned model. Equation (1) has been also analyzing by Maïna and co-workers for integer order derivatives (Maïna et al. 2015). A partial differential equation called an evolution equation shows how a physical system changes over time starting from given initial data. The used equation can be described as a nonlinear evolution equation because evolution equations are used in many fields of applied and engineering sciences Yokus et al. (2022).

1.1 Conformable derivative

Let $f : (0, \infty) \rightarrow \mathbb{R}$ be a function. Then, for all $t > 0$,

$$D_t^\alpha(f(t)) = \lim_{\epsilon \rightarrow 0} \frac{f(t + \epsilon t^{1-\alpha}) - f(t)}{\epsilon}$$

is called α , $0 < \alpha \leq 1$ order conformable fractional derivative of f (Khalil et al. 2014).

Some characteristics are given below:

Let $0 < \alpha \leq 1$, $\gamma > 0$, $a, b \in \mathfrak{R}$, and g, f α -differentiable at a point $t > 0$, then

- (i) $D_t^\alpha (af + b\bar{g}) = aD_t^\alpha (f) + bD_t^\alpha (g)$, for all $a, b \in \mathbb{R}$
- (ii) $D_t^\alpha (f g) = f D_t^\alpha (g) + g D_t^\alpha (f)$
- (iii) $D_t^\alpha (f \circ g(t)) = t^{1-\alpha} g'(t) f'(g(t))$.
- (iv) $D_t^\alpha (t^h) = h t^{h-\alpha}$, for all $h \in \mathbb{R}$
- (v) $D_t^\alpha (\delta) = 0$, where δ is constant.
- (vi) $D_t^\alpha (f/g) = \frac{g D_t^\alpha (f) - f D_t^\alpha (g)}{g^2}$.

Similarly, if f is differentiable, then $D_t^\alpha (f(t)) = t^{1-\alpha} \frac{df(t)}{dt}$.

2 Summary of the strategy

The used methods are inspired from the (w/g) -expansion procedure. Firstly, we consider a general nonlinear partial differential equation (NPDE) the form:

$$F(u, u_t, u_x, u_{tt}, u_{xt}, u_{xx}, \dots) = 0, \quad (2)$$

where x and t are independent variables, u is dependent variable. The following are the phases of the main technique:

1. If we apply the transformation $\xi = x - vt$, $u(x, t) = u(\xi)$ to Eq. (2), we transform Eq. (2) to the following ODE:

$$F(u, -vu', u', v^2 u'', -vu'', u'', \dots) = 0 \quad (3)$$

where $u' = \frac{du}{d\xi}$, v will be find out.

2. We assume the following solution for Eq. (3):

$$u(\xi) = \sum_{j=0}^M a_j \left(\frac{w}{g} \right)^j, \quad (4)$$

where a_j ($j = 0, \dots, M$) are constants which is going to be found out later. M is calculated by the use of homogeneous balance technique. This means, we balance the highest order derivatives and with the nonlinear terms in Eq. (3).

3. For w and g the following relation is given:

$$\left(\frac{w}{g} \right)' = a + b \left(\frac{w}{g} \right) + c \left(\frac{w}{g} \right)^2, \quad (5)$$

here a, b and c are arbitrary constants. One can discover that from Eq. (5):

$$w'g - wg' = ag^2 + bwg + cw^2. \quad (6)$$

4. Then, by substituting Eq. (4) into Eq. (3); by use of (5) and then by equating each coefficient of all powers of $(w/g)^j$ to zero, one may verify an equation system including a_j ($j = 0, \dots, M$), a, b, c and v .

5. From the solutions of these equations, one may obtain the values of a_j and v . After that, by substituting these values into (4), one finally obtain all possible solutions [?]. From now on, the customization of the (w/g) -expansion technique will be given and we have the following cases.

Case 1: From the substitution of $w = g'$, $a = -\mu$, $b = -\lambda$, $c = -1$ in (4) and (6), one may get the following results:

$$u(\xi) = \sum_{j=0}^M a_j \left(\frac{g'}{g}\right)^j$$

and g is the solution of:

$$g'' + \lambda g' + \mu g = 0.$$

This algorithm is called (G'/G) expansion method (Wang et al. 2008).

Case 2: From the substitution of $w = \tanh(\xi)$, $g = 1$, $a = 1$, $b = 0$, $c = -1$ in (4) and (6), we obtain:

$$u(\xi) = \sum_{j=0}^M a_j (\tanh(\xi))^j$$

and g is the solution of following equation:

$$(\tanh(\xi))' = 1 - (\tanh(\xi))^2.$$

Here is the \tanh -function method (Wazwaz 2005).

Case 3: From the substitution of $w = g'/g$, $b = 0$ in (4) and (6), a new form of solution may be rewritten as:

$$u(\xi) = \sum_{j=0}^M a_j \left(\frac{g'}{g^2}\right)^j \tag{7}$$

and the following second order ODE may be rewritten:

$$g''g^2 - 2gg'^2 = ag^4 + cg'^2, \tag{8}$$

which is called (g'/g^2) expansion procedure (Zayed and Arnous 2014).

Case 4: Surrogating $w = gg'$ in (4) and (6), to get:

$$u(\xi) = \sum_{i=0}^N a_i (g')^i \tag{9}$$

and the following equation can be rewritten:

$$g'' = a + bg' + cg'^2, \tag{10}$$

which is called as (g') expansion method (Akbulut et al. 2022).

2.1 Description of METHEM

In the current part of the paper, we will give demonstration of the main steps of METHEM. Assuming a conformable fractional nonlinear partial differential equation (CFNPDE):

$$G(g, g^2, \dots, \frac{\partial^\alpha g}{\partial t^\alpha}, \frac{\partial^{2\alpha} g}{\partial t^{2\alpha}}, \dots, \frac{\partial g}{\partial x}, \frac{\partial^2 g}{\partial x^2}, \dots) = 0. \quad (11)$$

where $g = g(x, t)$ shows the profile function. Assuming below travelling waves transformations:

$$g(x, t) = G(\zeta), \quad \zeta = \mu(x - v \frac{t^\alpha}{\alpha}) \quad (12)$$

where v represents the wave speed. From the substitution of Eq. (12) in Eq. (11), the following NLODE is obtained:

$$\chi(G, G^2, \mu G', \mu v^2 G'', \dots) = 0 \quad (13)$$

Assuming the root of Eq. (13) given below:

$$G(\zeta) = a_0 + \sum_{i=1}^N a_i \psi^i(\zeta) + \sum_{i=1}^N b_i \psi^{-i}(\zeta) \quad (14)$$

Here $a_0, a_i, b_i, (i = 1, 2, 3, \dots, N)$ are unknowns and it is necessary that both a_i and b_i are nonzero constants. Then from the utilization of the homogenous balance technique into Eq. (13), we obtain value of N .

Where $\psi(\zeta)$ fulfill the below equation:

$$\psi'(\zeta) = \Omega + \psi^2(\zeta) \quad (15)$$

where Ω is a constant and roots of Eq. (15) are given as Raslan et al. (2017):

Case 1: For $\Omega < 0$:

$$\psi(\zeta) = -\sqrt{-\Omega} \tanh(\sqrt{-\Omega} \zeta), \quad (16)$$

or

$$\psi(\zeta) = -\sqrt{-\Omega} \coth(\sqrt{-\Omega} \zeta). \quad (\text{Case 2:17})$$

For $\Omega = 0$:

$$\psi(\zeta) = \frac{-1}{\zeta} \quad (\text{Case 3:18})$$

: For $\Omega > 0$:

$$\psi(\zeta) = \sqrt{\Omega} \tan(\sqrt{\Omega} \zeta). \quad (19)$$

or

$$\psi(\zeta) = -\sqrt{\Omega} \cot(\sqrt{\Omega} \zeta). \quad (20)$$

By substituting of the Eq. (14) into Eq. (13) with Eq. (15), and by collecting the co-efficient of $\psi(\zeta)$ for each order and inserting each order equal to 0, a set of algebraic equations having $a_0, a_i, b_i (i = 1, 2, 3, \dots, N)$, and Ω is obtained to solve by using symbolic computation algorithms. Then, we solve the system to get the results of Eq. (11).

2.2 Modified $(\frac{G'}{G^2})$ -expansion method

Assuming (1+1)-dimensional conformable fractional PDE of the form

$$H(u, u^2, \dots, \frac{\partial^\alpha u}{\partial t^\alpha}, \frac{\partial^{2\alpha} u}{\partial t^{2\alpha}}, \dots, \frac{\partial u}{\partial x}, \frac{\partial^2 u}{\partial x^2}, \dots) = 0, \tag{21}$$

where $u(x, t)$ represents a wave profile.

The modified $(\frac{G'}{G^2})$ -expansion procedure will be performed to find analytical results of Eq. (21). Now, steps of modified $(\frac{G'}{G^2})$ -expansion technique will be described (Zafar et al. 2020):

Step 1 By applying the travelling wave transformation

$$\zeta = \mu \left(x - v \frac{t^\alpha}{\alpha} \right), \quad u(x, t) = U(\zeta), \tag{22}$$

Equation (21) changed into resulting nonlinear ODE:

$$N(U, U_\zeta, U_{\zeta\zeta}, \dots) = 0, \tag{23}$$

where $U = \frac{dU}{d\zeta}, U_{\zeta\zeta} = \frac{d^2U}{d\zeta^2}, \dots$

Step 2 Assuming roots of Eq.(13) given as:

$$U(\zeta) = \sum_{i=0}^m d_i \left(\frac{G'}{G^2}\right)^i, \tag{24}$$

where $d_i (i = 0, 1, 2, \dots, m)$ are un-governed that to be find out later with factor $d_m \neq 0$.

A function $G=G(\zeta)$ fulfill the below differential equation,

$$\left(\frac{G'}{G^2}\right)' = \Delta \left(\frac{G'}{G^2}\right)^2 + \Xi, \tag{25}$$

where Ξ and Δ are the un-governed parameters. Equation (25) has the following solutions:

When $\Xi\Delta < 0$,

$$\left(\frac{G'}{G^2}\right) = -\frac{\sqrt{|\Xi\Delta|}}{\Delta} + \frac{\sqrt{|\Xi\Delta|}}{2} \left[\frac{c_1 \sinh(\sqrt{\Xi\Delta} \zeta) + c_2 \cosh(\sqrt{\Xi\Delta} \zeta)}{c_1 \cosh(\sqrt{\Xi\Delta} \zeta) + c_2 \sinh(\sqrt{\Xi\Delta} \zeta)} \right], \tag{26}$$

When $\Xi\Delta > 0$,

$$\left(\frac{G'}{G^2}\right) = \sqrt{\frac{\Xi}{\Delta}} \left[\frac{c_1 \cos(\sqrt{\Xi\Delta} \zeta) + c_2 \sin(\sqrt{\Xi\Delta} \zeta)}{c_1 \sin(\sqrt{\Xi\Delta} \zeta) - c_2 \cos(\sqrt{\Xi\Delta} \zeta)} \right], \tag{27}$$

When $\Xi = 0$ and $\Delta \neq 0$,

$$\left(\frac{G'}{G^2}\right) = -\frac{c_1}{\Delta(c_1\zeta + c_2)}. \quad (28)$$

Where c_1 and c_2 are the constants.

Step 3 Substituting Eq. (24) into Eq. (23) with Eq. (25) and setting all the constants of each power of $\left(\frac{G'}{G^2}\right)^i$ equal to zero, and by solving the obtained sets of equations, we get the solutions.

Step 4 Substituting Eq. (24) of which d_i, Δ, ν has been find out in the Step 3 into Eq. (22), we find the traveling wave roots of Eq. (21).

3 Applications

3.1 Application to the METHEM

In this section, we will give the applications of the METHEM to the Eq. (1). We will consider the following travelling wave transformation:

$$v(x, t) = V(\xi), \quad \text{where } \xi = \kappa \left(x - \frac{\lambda t^\alpha}{\alpha} \right) \quad (29)$$

By using the Eq. (29) into Eq. (1), we get

$$\begin{aligned} -\lambda\kappa R_f CV' - \kappa^2\sigma^2 M[(1-\eta)V'' - \eta U''] + \gamma[V^3 - (1+a)V^2 + aV] &= 0 \\ -\lambda\kappa R_f CU' - \kappa^2\sigma^2 M[(1-\eta)U'' - \eta V''] + \gamma[U^3 - (1+a)U^2 + aU] &= 0 \end{aligned} \quad (30)$$

If we use of homogeneous balance technique into Eq. (30), we achieve $N = 1$. Therefore Eq. (14) changes in to:

$$\begin{aligned} V(\xi) &= a_0 + a_1\psi(\xi) + b_1\psi(\xi)^{-1} \\ U(\xi) &= f_0 + f_1\psi(\xi) + d_1\psi(\xi)^{-1} \end{aligned} \quad (31)$$

From the substitution of Eq. (31) into Eq. (30) with Eq. (15), a system of algebraic equations in terms of $a_0, a_1, b_1, f_0, f_1, \lambda$ and Ω is obtained. Using Mathematica software program, we can obtain the following solutions:

Set I:

$$\left\{ a_0 = f_0 = \frac{1}{2}, a_1 = f_1 = 0, b_1 = d_1 = \mp \frac{i\sqrt{\gamma}}{4\sqrt{2}\sqrt{2\eta-1}\kappa\sqrt{M\sigma}}, \right. \\ \left. \lambda = \mp \frac{i(2a-1)\sqrt{\gamma}\sqrt{2\eta-1}\sqrt{M\sigma}}{\sqrt{2}CR_f}, \Omega = \frac{\gamma}{8(2\eta-1)\kappa^2M\sigma^2} \right\} \quad (32)$$

if $\Omega < 0$, then by putting Eqs. (32) and (16) in Eq.(31), we gain:

$$v_1(x, t) = u_1(x, t) = \frac{1}{2} \left(1 \pm \coth \left(\frac{\xi \sqrt{\frac{\gamma}{\kappa^2 \sigma^2 (M - 2\eta M)}}}{2\sqrt{2}} \right) \right) \tag{33}$$

or by substituting Eqs. (32) and (17) in Eq. (31), we get:

$$v_2(x, t) = u_2(x, t) = \frac{1}{2} \left(1 \pm \tanh \left(\frac{\xi \sqrt{\frac{\gamma}{\kappa^2 \sigma^2 (M - 2\eta M)}}}{2\sqrt{2}} \right) \right) \tag{34}$$

Figure 1 represents graph of $v_1(x, t)$ for Eq. (33) and this figure called periodic.

If $\Omega > 0$, then by substituting Eqs. (32) and (19) in Eq. (31), we can find:

$$v_3(x, t) = u_3(x, t) = \frac{1}{2} \left(1 \mp i \cot \left(\frac{\xi \sqrt{\frac{\gamma}{(2\eta - 1)\kappa^2 M \sigma^2}}}{2\sqrt{2}} \right) \right) \tag{35}$$

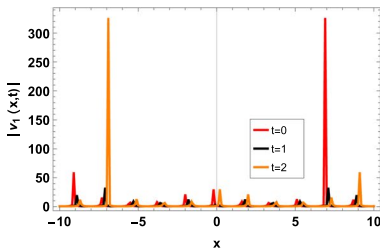
or

by substituting Eqs. (32) and (20) in Eq. (31), we may get:

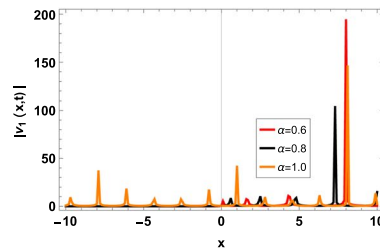
$$v_4(x, t) = u_4(x, t) = \frac{1}{2} \left(1 \pm i \tan \left(\frac{\xi \sqrt{\frac{\gamma}{(2\eta - 1)\kappa^2 M \sigma^2}}}{2\sqrt{2}} \right) \right) \tag{36}$$

Figure 2 represents graph of $v_2(x, t)$ for Eq. (34) and this figure called kink shape wave.

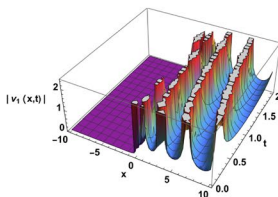
Set 2:



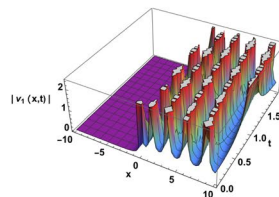
(a) 2D plot for different values of t



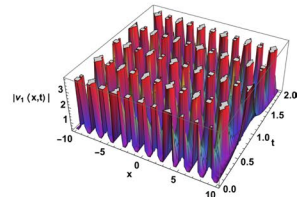
(b) 2D plot for different values of α



(c) $\alpha = 0.6$



(d) $\alpha = 0.8$



(e) $\alpha = 1$

Fig. 1 Graph of $v_1(x, t)$ for Eq. (33)

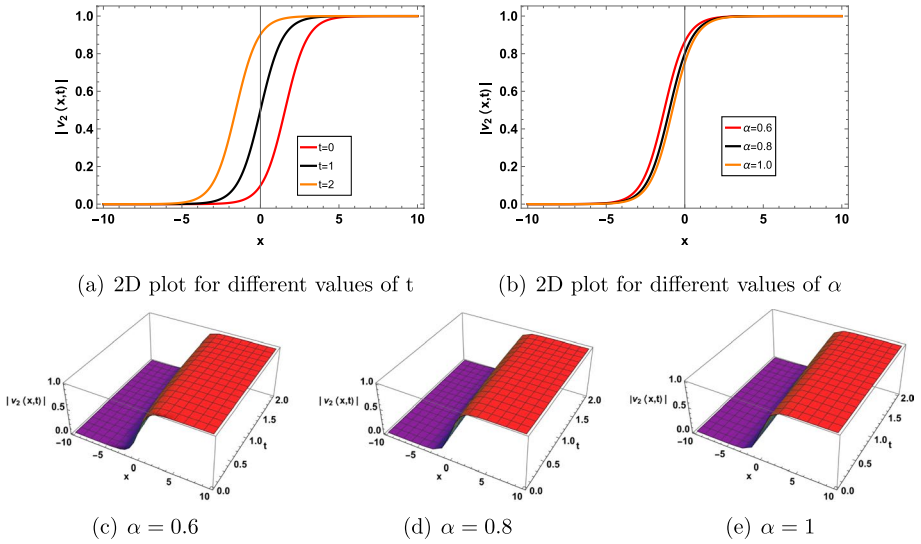


Fig. 2 Graph of $v_2(x, t)$ for Eq. (34)

$$\left\{ a_0 = f_0 = \frac{1}{2}, a_1 = f_1 = \pm \frac{i\sqrt{2}\sqrt{2\eta-1}\kappa\sqrt{M}\sigma}{\sqrt{\gamma}}, b_1 = d_1 = \mp \frac{i\sqrt{\gamma}}{16\sqrt{2}\sqrt{2\eta-1}\kappa\sqrt{M}\sigma}, \right.$$

$$\left. \lambda = \mp \frac{i(2a-1)\sqrt{\gamma}\sqrt{2\eta-1}\sqrt{M}\sigma}{\sqrt{2}CR_f}, \omega = \frac{\gamma}{32(2\eta-1)\kappa^2M\sigma^2} \right\} \tag{37}$$

Set 3:

$$\left\{ a_0 = f_0 = \frac{1}{2}, a_1 = f_1 = \mp \frac{i\sqrt{2}\sqrt{2\eta-1}\kappa\sqrt{M}\sigma}{\sqrt{\gamma}}, b_1 = d_1 = 0, \right.$$

$$\left. \lambda = \pm \frac{i(2a-1)\sqrt{\gamma}\sqrt{2\eta-1}\sqrt{M}\sigma}{\sqrt{2}CR_f}, \Omega = \frac{\gamma}{8(2\eta-1)\kappa^2M\sigma^2} \right\} \tag{38}$$

Set 4:

$$\left\{ a_0 = f_0 = \frac{a+1}{2}, a_1 = f_1 = -\frac{\sqrt{2}(a-1)^2}{\sqrt{-\frac{(a-1)^4\gamma}{(2\eta-1)\kappa^2M\sigma^2}}}, b_1 = d_1 = -\frac{\sqrt{-\frac{(a-1)^4\gamma}{(2\eta-1)\kappa^2M\sigma^2}}}{16\sqrt{2}}, \right.$$

$$\left. \lambda = -\frac{(a-1)^2(a+1)\gamma}{\sqrt{2}C\kappa R_f \sqrt{-\frac{(a-1)^4\gamma}{(2\eta-1)\kappa^2M\sigma^2}}}, \Omega = \frac{(a-1)^2\gamma}{32(2\eta-1)\kappa^2M\sigma^2} \right\} \tag{39}$$

Set 5:

$$\{a_0 = f_0 = \frac{a+1}{2}, a_1 = f_1 = + \frac{\sqrt{2}(a-1)^2}{\sqrt{-\frac{(a-1)^4\gamma}{(2\eta-1)\kappa^2 M\sigma^2}}}, b_1 = d_1 = + \frac{\sqrt{-\frac{(a-1)^4\gamma}{(2\eta-1)\kappa^2 M\sigma^2}}}{16\sqrt{2}},$$

$$\lambda = + \frac{(a-1)^2(a+1)\gamma}{\sqrt{2}C\kappa R_f \sqrt{-\frac{(a-1)^4\gamma}{(2\eta-1)\kappa^2 M\sigma^2}}}, \Omega = \frac{(a-1)^2\gamma}{32(2\eta-1)\kappa^2 M\sigma^2} \}$$
(40)

Set 6:

$$\{a_0 = f_0 = \frac{a+1}{2}, a_1 = f_1 = 0, b_1 = d_1 = \mp \frac{\sqrt{-\frac{(a-1)^4\gamma}{(2\eta-1)\kappa^2 M\sigma^2}}}{4\sqrt{2}},$$

$$\lambda = \mp \frac{(a-1)^2(a+1)\gamma}{\sqrt{2}C\kappa R_f \sqrt{-\frac{(a-1)^4\gamma}{(2\eta-1)\kappa^2 M\sigma^2}}}, \Omega = \frac{(a-1)^2\gamma}{8(2\eta-1)\kappa^2 M\sigma^2} \}$$
(41)

Set 7:

$$\{a_0 = f_0 = \frac{a+1}{2}, a_1 = f_1 = \mp \frac{i\sqrt{2}\sqrt{2\eta-1}\kappa\sqrt{M}\sigma}{\sqrt{\gamma}}, b_1 = d_1 = 0,$$

$$\lambda = \mp \frac{i(a+1)\sqrt{\gamma}\sqrt{2\eta-1}\sqrt{M}\sigma}{\sqrt{2}CR_f}, \omega = \frac{(a-1)^2\gamma}{8(2\eta-1)\kappa^2 M\sigma^2} \}$$
(42)

Set 8:

$$\{a_0 = f_0 = \frac{a}{2}, a_1 = f_1 = \pm \frac{i\sqrt{2}\sqrt{2\eta-1}\kappa\sqrt{M}\sigma}{\sqrt{\gamma}}, b_1 = d_1 = \mp \frac{ia^2\sqrt{\gamma}}{16\sqrt{2}\sqrt{2\eta-1}\kappa\sqrt{M}\sigma},$$

$$\lambda = \pm \frac{i(a-2)\sqrt{\gamma}\sqrt{2\eta-1}\sqrt{M}\sigma}{\sqrt{2}CR_f}, \Omega = \frac{a^2\gamma}{32(2\eta-1)\kappa^2 M\sigma^2} \}$$
(43)

Set 9:

$$\{a_0 = f_0 = \frac{a}{2}, a_1 = f_1 = 0, b_1 = d_1 = \mp \frac{ia^2\sqrt{\gamma}}{4\sqrt{2}\sqrt{2\eta-1}\kappa\sqrt{M}\sigma},$$

$$\lambda = \pm \frac{i(a-2)\sqrt{\gamma}\sqrt{2\eta-1}\sqrt{M}\sigma}{\sqrt{2}CR_f}, \Omega = \frac{a^2\gamma}{8(2\eta-1)\kappa^2 M\sigma^2} \}$$
(44)

Set 10:

$$\left\{ \begin{aligned} a_0 = f_0 = \frac{a}{2}, a_1 = f_1 = \mp \frac{i\sqrt{2}\sqrt{2\eta-1}\kappa\sqrt{M}\sigma}{\sqrt{\gamma}}, b_1 = d_1 = 0, \\ \lambda = \mp \frac{i(a-2)\sqrt{\gamma}\sqrt{2\eta-1}\sqrt{M}\sigma}{\sqrt{2}CR_f}, \Omega = \frac{a^2\gamma}{8(2\eta-1)\kappa^2M\sigma^2} \end{aligned} \right\} \tag{45}$$

3.2 Application to the modified $(\frac{G'}{G^2})$ -expansion method

For $N = 1$, Eq. (24) changes to:

$$\begin{aligned} V(\xi) &= d_0 + d_1\left(\frac{G'}{G^2}\right) \\ U(\xi) &= f_0 + f_1\left(\frac{G'}{G^2}\right) \end{aligned} \tag{46}$$

Putting Eq. (46) into Eq. (30) with Eq. (25), we achieve sets of algebraic equations in terms of $d_0, d_1, f_0, f_1, \lambda$ and κ . Using the Mathematica software program, we can find the following results:

Set 1:

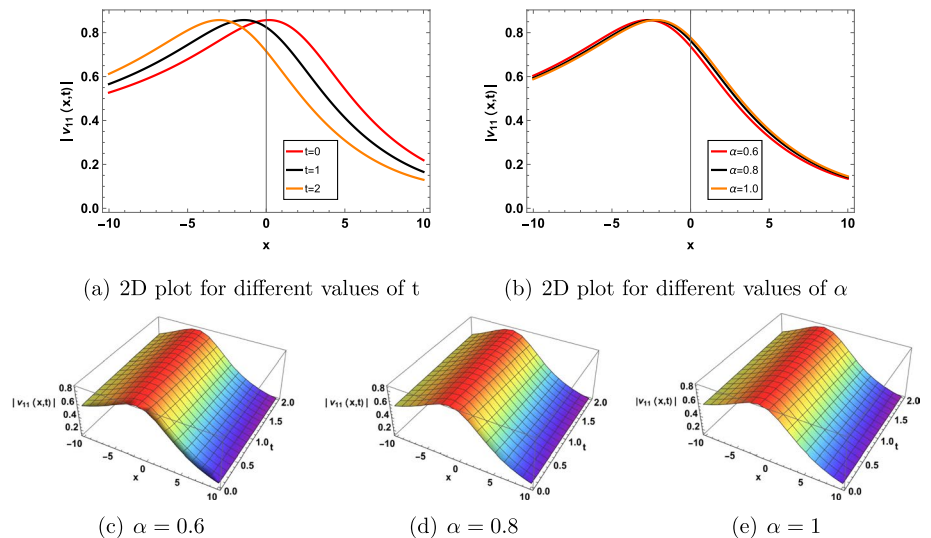


Fig. 3 Graph of $v_{11}(x, t)$ for Eq. (48)

$$\left. \begin{aligned} \{d_0 = f_0 = \frac{1}{2}, d_1 = f_1 = \mp \frac{i\sqrt{\Delta}}{2\sqrt{\Xi}}, \lambda = \mp \frac{(1-2a)\sqrt{\gamma}\sqrt{\Delta(2\eta-1)(-M)\Xi\sigma^2}}{\sqrt{2c}\sqrt{\Delta}\sqrt{\Xi}R_f}, \\ \kappa = -\frac{i\sqrt{\gamma}}{\sqrt{8\Delta M\Xi\sigma^2 - 16\Delta\eta M\Xi\sigma^2}} \} \end{aligned} \right\} \tag{47}$$

When $\Xi\Delta < 0$,

$$v_{11}(x, t) = u_{11}(x, t) = \frac{1}{2} - \frac{i\sqrt{\Delta}}{2\sqrt{\Xi}} \left[-\frac{\sqrt{|\Xi\Delta|}}{\Delta} + \frac{\sqrt{|\Xi\Delta|}}{2} \left[\frac{c_1 \sinh(\sqrt{\Xi\Delta} \xi) + c_2 \cosh(\sqrt{\Xi\Delta} \xi)}{c_1 \cosh(\sqrt{\Xi\Delta} \xi) + c_2 \sinh(\sqrt{\Xi\Delta} \xi)} \right] \right], \tag{48}$$

Figure 3 represents graph of $v_{11}(x, t)$ for Eq. (48).

When $\Xi\Delta > 0$,

$$v_{12}(x, t) = u_{12}(x, t) = \frac{1}{2} - \frac{i\sqrt{\Delta}}{2\sqrt{\Xi}} \left[\sqrt{\frac{\Xi}{\Delta}} \left[\frac{c_1 \cos(\sqrt{\Xi\Delta} \xi) + c_2 \sin(\sqrt{\Xi\Delta} \xi)}{c_1 \sin(\sqrt{\Xi\Delta} \xi) - c_2 \cos(\sqrt{\Xi\Delta} \xi)} \right] \right], \tag{49}$$

Figure 4 represents graph of $v_{12}(x, t)$ appears in Eq. (49) and this figure called singular bell shape wave.

Where c_1 and c_2 are arbitrary constants.

Set 2:

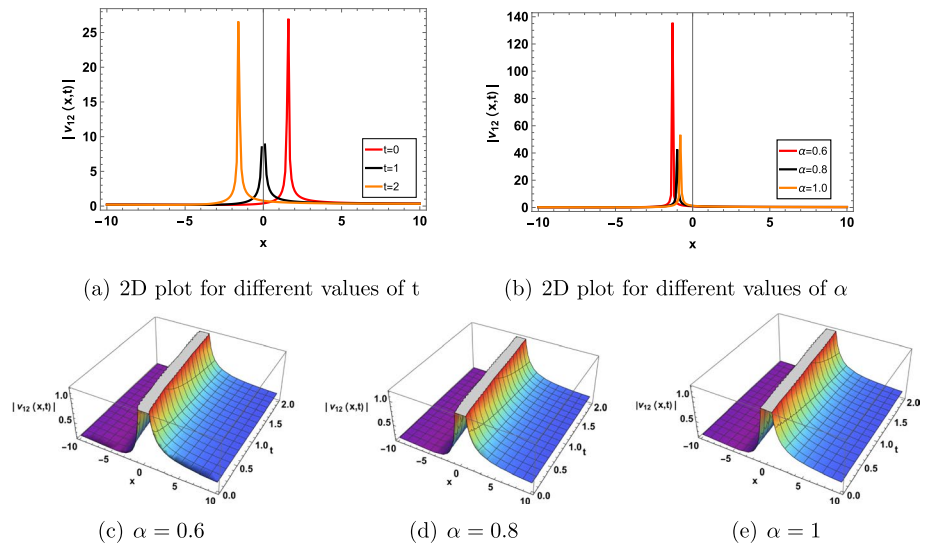


Fig. 4 Wave profile of $v_{12}(x, t)$ appears in Eq. (49)

$$\left. \begin{aligned} \{d_0 = f_0 = \frac{a+1}{2}, d_1 = f_1 = \mp \frac{1}{2} \sqrt{-\frac{(a-1)^2 \Delta}{\Xi}}, \\ \lambda = \mp \frac{i(a-1)(a+1) \sqrt{\gamma} \sqrt{\Delta(2\eta-1)(-M)\Xi\sigma^2}}{\sqrt{2c\Xi R_f} \sqrt{-\frac{(a-1)^2 \Delta}{\Xi}}}, \\ \kappa = -\frac{i(a-1) \sqrt{\gamma}}{\sqrt{8\Delta M \Xi \sigma^2 - 16\Delta \eta M \Xi \sigma^2}} \} \end{aligned} \right\} \quad (50)$$

Set 3:

$$\left. \begin{aligned} \{d_0 = f_0 = \frac{a}{2}, d_1 = f_1 = \mp \frac{ia\sqrt{\Delta}}{2\sqrt{\Xi}}, \lambda = \mp \frac{(a-2) \sqrt{\gamma} \sqrt{\Delta(2\eta-1)(-M)\Xi\sigma^2}}{\sqrt{2c\sqrt{\Delta}\sqrt{\Xi}R_f}}, \\ \kappa = -\frac{ia\sqrt{\gamma}}{\sqrt{8\Delta M \Xi \sigma^2 - 16\Delta \eta M \Xi \sigma^2}} \} \end{aligned} \right\} \quad (51)$$

4 Discussion and results

In the current manuscript, we applied two different techniques which are called modified extended tanh expansion and modified $(\frac{G'}{G^2})$ -expansion methods to the coupled nerve fibers model. The obtained results are different from previous results in literature. The obtained results are given as trigonometric, hyperbolic and exponential functions. Then in Fig. 1, we plotted the first solution obtained using method modified extended tanh expansion method. Firstly, we plotted 2D figure for different value of t in Fig. 1a, b is plotted for different values of α . Secondly, we plotted 3D in Fig. 1c–e for different values of α . Finally, we say Fig. 1 represents periodic solutions. With the same procedure, we plotted the solution Eq. (34) in Fig. 2 represents kink shape wave profile. All the plotted figures are different from each other. If we substitute different values of t and α in the results, the motion of the wave does not change.

5 Conclusion

We have succeed to obtain the modernistic solitary wave solutions of coupled nerve fibers model along novel definition of derivative by utilizing the modified extended tanh expansion function and modified $(\frac{G'}{G^2})$ -expansion methods. Used auxiliary ordinary differential equations are different from each other in the methods. So, the solutions of the auxiliary equations are different from each other. The obtained solutions have been verified and demonstrated via the graphical representations by using software programmes. At the end, it is concluded that, to solve other CFNPDEs, the modified extended tanh expansion and modified $(\frac{G'}{G^2})$ -expansion techniques are very reliable, straightforward, and helpful. The used methods are powerful for constructing the exact solutions of the fractional order differential equations. Also, it's easy to apply methods to equations and we obtain the different solutions from each other.

Author contributions The study's conception and design were the result of contributions from all the authors. WR and MR wrote the main manuscript, AZ prepared figures, AA and MK revised the paper. The analysis of the results was done by all authors. All the authors read and approved the final manuscript.

Funding There has been no significant financial support for this work.

Data availability The data and materials used have been incorporated into the manuscript.

Declarations

Conflict of interest Our intention is to verify that there are no conflicts of interest that have been identified in relation to this publication.

References

- Ablowitz, M.J., Clarkson, P.A.: *Soliton. Nonlinear Evolution Equations and Inverse Scattering*, Cambridge University Press, New York (1991)
- Akbulut, A., Islam, S.M.R., Rezazadeh, H., Tascan, F.: Obtaining exact solutions of nonlinear partial differential equations via two different methods. *Int. J. Mod. Phys. B* **36**(5), 2250041 (2022)
- Ali, M.S., Saravanan, S.: Finite-time stability for memristor based uncertain neural networks with time-varying delays-via average dwell time approach. *Chin. J. Phys.* **55**(5), 1953–1971 (2017)
- Duran, S., Yokus, A., Durur, H.: Surface wave behavior and refraction simulation on the ocean for the fractional Ostrovsky-Benjamin-Bona-Mahony equation. *Mod. Phys. Lett. B* **35**(31), 2150477 (2021)
- Duran, S., Yokus, A., Durur, H., Kaya, D.: Refraction simulation of internal solitary waves for the fractional Benjamin-Ono equation in fluid dynamics. *Mod. Phys. Lett. B* **35**(26), 2150363 (2021)
- El-Shiekh, R.M., Gaballah, M.: New rogon waves for the nonautonomous variable coefficients Schrödinger equation. *Opt. Quant. Electron.* **53**(8), 1–12 (2021)
- Hirota, R.: Exact solution of the Korteweg-de Vries equation for multiple collisions of solitons. *Phys. Rev. Lett.* **27**, 1192–1194 (1971)
- Huang, Shoufang, Zhang, Jiqian, Wang, Maosheng, Hu, Chin-Kun.: Firing patterns transition and desynchronization induced by time delay in neural networks. *Phys. A* **499**, 88–97 (2018)
- Kalim, U.T., Younis, M., Rezazadeh, H., Rizvi, S.T.R., Osman, M.S.: Optical solitons with quadratic-cubic nonlinearity and fractional temporal evolution. *Mod. Phys. Lett. B* **1850317**, 1–13 (2018)
- Khalil, R., Al-Horani, M., Yousef, A., Sababheh, M.: A new definition of fractional derivative. *J. Comput. Appl. Math.* **264**, 65–70 (2014)
- Ly, Z.-S., Zhu, C.-P., Nie, P., Zhao, J., Yang, H.-J., Wang, Y.-J., Hu, C.-K.: Exponential distance distribution of connected neurons in simulations of two-dimensional in vitro neural network development. *Front. Phys.* **12**(3), 128902 (2017)
- Maïna, I., Tabi, C.B., Ekobena-Fouda, H.P., Mohamadou, A., Kofané, T.C.: Discrete impulses in ephaptically coupled nerve fibers. *Chaos Interdiscip. J. Nonlinear Sci.* **25**(4), 043118 (2015)
- Mathanaranjan, T., Kumar, D., Rezazadeh, H., Akinyemi, L.: Optical solitons in metamaterials with third and fourth order dispersions. *Opt. Quant. Electron.* **54**(5), 1–15 (2022)
- Moore, J.W., Joyner, R.W., Brill, M.H., Waxman, S.D., Najjar-Joa, M.: Simulations of conduction in uniform myelinated fibers. Relative sensitivity to changes in nodal and internodal parameters. *Biophys. J.* **21**(2), 147–160 (1978)
- Osman, M.S., Machado, J.A.T., Baleanu, D., Zafar, A., Raheel, M.: On distinctive solitons type solutions for some important nonlinear Schrödinger equations. *Opt. Quant. Electron.* **53**(2), 1–24 (2021)
- Raslan, K.R., Khalid, K.A., Shallal, M.A.: The modified extended tanh method with the Riccati equation for solving the space-time fractional EW and MEW equations. *Chaos Solitons Fract.* **103**, 404–409 (2017)
- Rezazadeh, H., Osman, M.S., Eslami, M., Ekici, M., Abdullah, S., Mir, A., Othman, W.A.M., Wong, B.R., Mohammad, M., Zhou, Q., Biswas, A., Belic, M.: Mitigating internet bottleneck with fractional temporal evolution of optical solitons having quadratic-cubic nonlinearity. *Optik* **164**, 84–92 (2018)
- Tala-Tebue, E., Djoufack, Z.I., Djimeli-Tsajio, A., Kenfack-Jiotsa, A.: Solitons and other solutions of the nonlinear fractional Zoomeron equation. *Chin. J. Phys.* **56**, 1232–1246 (2018)
- Tala-Tebue, Eric, Rezazadeh, Hadi, Eslami, Mostafa, Bekir, Ahmet: New approach to model coupled nerve fibers and exact solutions of the system. *Chin. J. Phys.* **62**, 179–186 (2019)

- Tourani, S., Rahmani, Z., Rezaie, B.: Adaptive observer-based projective synchronization for chaotic neural networks with mixed time delays. *Chin. J. Phys.* **54**(2), 285–297 (2016)
- Tsai, Kuo-Ting., Hu, Chin-Kun., Li, Kuan-Wei., Hwang, Wen-Liang., Chou, Ya-Hui.: Circuit variability interacts with excitatory-inhibitory diversity of interneurons to regulate network encoding capacity. *Sci. Rep.* **8**(1), 1–15 (2018)
- Wang, M., Li, X., Zhang, J.: The $(\frac{G}{G})$ -expansion method and travelling wave solutions of nonlinear evolution equations in mathematical physics. *Phys. Lett. A* **372**(4), 417–423 (2008)
- Wazwaz, A.M.: The tanh method: solitons and periodic solutions for the Dodd-Bullough-Mikhailov and the Tzitzeica-Dodd-Bullough equations. *Chaos Solitons Fract.* **25**, 55–63 (2005)
- Weiss, J., Tabor, M., Carnevale, G.: The painleve property for partial differential equations. *J. Math. Phys.* **24**, 522–526 (1983)
- Yokus, A., Durur, H., Duran, S., Islam, T.: Ample felicitous wave structures for fractional foam drainage equation modeling for fluid-flowmechanism. *Comput. Appl. Math.* **41**, 174 (2022)
- Yokus, A., Duran, S., Durur, H.: Analysis of wave structures for the coupled Higgs equation modelling in the nuclear structure of an atom. *Eur. Phys. J. Plus* **137**, 992 (2022)
- Zafar, A., Bekir, A., Raheel, M., Razzaq, W.: Optical soliton solutions to Biswas-Arshed model with truncated M-fractional derivative. *Optik* **222**, 165355 (2020)
- Zafar, A., Raheel, M., Rezazadeh, H., Mustafa, A., Mehmet, A.: New chirp-free and chirped form optical solitons to the non-linear Schrödinger equation. *Opt. Quant. Electron.* **53**(11), 1–19 (2021)
- Zayed, E.M.E., Arnous, A.H.: The modified (w/g) -expansion method and its applications for solving the modified generalized Vakhnenko equation. *Ital. J. Pure Appl. Math.* **32**, 477–492 (2014)
- Zayed, E.M., Shohib, R.M., Alngar, M.E.: Optical solitons in Bragg gratings fibers for the nonlinear (2+1)-dimensional Kundu-Mukherjee-Naskar equation using two integration schemes. *Opt. Quant. Electron.* **54**(1), 16 (2022)

Publisher's Note Springer Nature remains neutral with regard to jurisdictional claims in published maps and institutional affiliations.

Springer Nature or its licensor (e.g. a society or other partner) holds exclusive rights to this article under a publishing agreement with the author(s) or other rightsholder(s); author self-archiving of the accepted manuscript version of this article is solely governed by the terms of such publishing agreement and applicable law.